TR-LIF LIFETIME MEASUREMENTS AND HFR+CPOL CALCULATIONS OF RADIATIVE PARAMETERS IN VANADIUM ATOM (V I)

Q. Wang[1,2], L. Y. Jiang[1,2], P. Quinet[3,4], P. Palmeri[3], W. Zhang[3], X. Shang[1,2], Y. S. Tian[1,2], and Z. W. Dai[1,2]

[1] College of Physics, Jilin University, Changchun 130012, China; dai@jlu.edu.cn
[2] Key Lab of Coherent Light, Atomic and Molecular Spectroscopy, Ministry of Education, Changchun 130012, China
[3] Astrophysique et Spectroscopie, Université de Mons—UMONS, 20 Place du Parc, B-7000 Mons, Belgium; Pascal.quinet@umons.ac.be
[4] IPNAS, Université de Liège, B-4000 Liège, Belgium

ABSTRACT

Radiative lifetimes of 79 levels belonging to the $3d^3 4s4p$, $3d^4 4p$, $3d^3 4s5p$, $3d^4 5p$, and $3d^3 4s4d$ configurations of V I with energy from 26,604.807 to 46,862.786 cm^{-1} have been measured using time-resolved laser-induced fluorescence (TR-LIF) spectroscopy in laser-produced plasma. The lifetime values reported in this paper are in the range of 3.3–494 ns, and the uncertainties of these measurements are within ±10%. A good agreement was obtained with previous data. HFR+CPOL calculations have been performed and used to combine the calculated branching fractions with the available experimental lifetimes to determine semi-empirical transition probabilities for 784 V I transitions.

Key words: atomic data – methods: laboratory: atomic – techniques: spectroscopic

Online-only material: machine-readable table

1. INTRODUCTION

The determination of elemental abundances and their patterns in stellar atmospheres has recently challenged the accuracy of the oscillator strengths used in stellar spectrum modeling. More precisely, an accuracy of the order of ∼0.05 dex in differential abundances (and therefore also in log *gf*) is needed to detect the effect of planet formation in the stellar atmospheres (Meléndez et al. 2009; Ramírez et al. 2014). These effects are marked by a ∼20% depletion of refractory elements with respect to the volatile elements. Vanadium ($Z = 23$) is a refractory element that belongs to the iron group. Due to its complex electronic structure related to an open $3d$ subshell and a relatively high cosmic abundance, e.g., $\varepsilon_V = \log(N_V/N_H) + 12 = 3.93 \pm 0.08$ in the Sun (Asplund et al. 2009), many lines of V I and V II are observed in solar and stellar spectra. Experimental oscillator strengths are essential for the determination of elemental abundances but direct measurements of oscillator strengths are difficult (Den Hartog et al. 2011; Larsson 1994). A reliable and convenient method for obtaining experimental oscillator strengths is through the combination of measured radiative lifetimes with accurate branching fractions (BFs). Hence, the measurements of lifetimes and BFs are of great significance.

Roberts et al. (1973) measured radiative lifetimes for 14 levels of V I in the energy range 21,963.45–40,535.70 cm^{-1} using the beam-foil technique. Rudolph & Helbig (1982) measured the lifetimes of nine levels of V I using a selective pulsed laser excitation in an atomic beam produced by a special cage formed with tungsten and vanadium wire. Doerr et al. (1985) reported 12 lifetimes of V I levels by selective laser excitation of an atomic beam produced by thermal evaporation of vanadium metal. Later on, Whaling et al. (1985) combined their time-resolved laser-induced fluorescence (TR-LIF) lifetimes obtained for 39 odd-parity levels with their Fourier transform spectroscopic BFs to determine absolute transition probabilities for 208 V I lines in the spectral range 318–1640 nm. More recently, Xu et al. (2006) measured 10 lifetimes of V I in

the energy range 30,635.59–41,928.48 cm^{-1} using the TR-LIF experimental method.

The lifetimes of highly excited V I energy levels ($E > 27,000$ cm^{-1}) available in the literature are relatively scarce. Moreover, there are still differences between some measurements that go beyond their error bars. These have motivated the present TR-LIF lifetime measurements of the 79 highly excited levels ranging from 26,604.807 to 46,862.786 cm^{-1}. In addition, HFR+CPOL calculations have been carried out to provide BFs in order to obtain the absolute semi-empirical radiative rates for 784 V I lines.

2. EXPERIMENTAL SETUP

The time-resolved laser spectroscopic methods can selectively excite specific atomic levels using tunable lasers and reduce the influence of cascade effects on the measured radiative lifetimes. This technique has already proven its reliability and efficiency and has been used many times with success by many groups around the world (Doerr et al. 1985; Den Hartog et al. 2011; Xu et al. 2006). The experimental setup used for the lifetime measurement is similar to that described in our previous papers (Feng et al. 2010; Zhang et al. 2010), and so only a brief description is given here.

A 532 nm Nd:YAG laser with a 8 ns pulse duration emitted with 10 Hz repetition rate and an energy of 5–10 mJ was focused on a rotating vanadium foil in a vacuum chamber through a 30 cm focal-length lens to produce laser-induced plasma. The latter, employed as a free-atom source, supplied sufficient numbers of V atoms in the ground and in some metastable states. In order to obtain a tunable excitation pulse, another Nd:YAG laser with characteristics similar to the ablation pulse was used to pump a dye laser (Sirah Cobra-Stretch) in which DCM dye operated. The second-order harmonic of the dye laser produced by a beta barium borate (BBO) crystal was focused into a stimulated Raman scattering cell with H_2 at 15 bars to obtain the first-order Stokes component of Raman shifting. The third-order harmonic of the dye laser was obtained with the use of two BBO crystals and a retarding plate. Thus, the wavelength
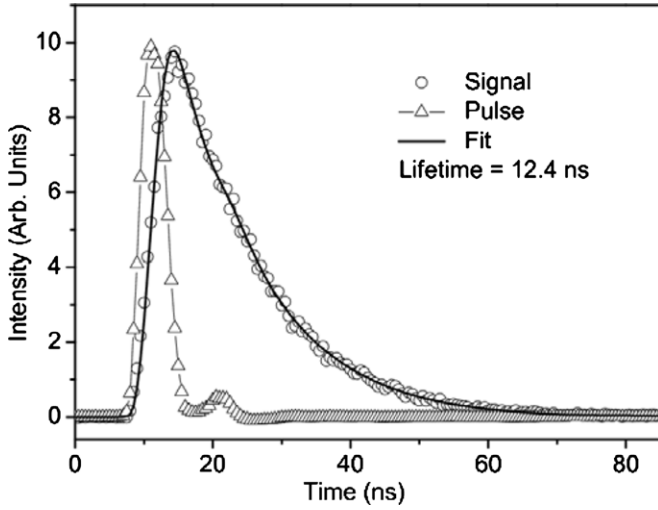
Figure 1. Typical fluorescence decay curve of the 42,245.489 cm^{-1} level of V I with the fitted convolution curve between the laser pulse and an exponential.

Figure 2. Typical fluorescence decay curve of the 31317.440 cm^{-1} level of V I with an exponential fit for lifetime evaluation.

of the excitation pulse is tunable in the range 210–380 nm. The excitation pulse with about 6 ns duration was sent horizontally into the vacuum chamber about 8 mm above the sample to excite free V atoms. The delay time between the ablation and excitation pulses was adjusted by a digital delay generator (SRS DG535). The fluorescence emitted from the measured levels was imaged by a fused silica lens and focused into a grating monochromator ($f = 10$ cm) for dispersion and then detected by a microchannel plate photomultiplier tube (Hamamatsu R3809U-58) with a 163 ps rise time. A 2.5 GHz digital oscilloscope (Tektronix DPO7254) was used to register and average the transient signals from the detector.

In order to wash out quantum beats produced by the Earth's magnetic field and reduce the recombination background from the plasma, an appropriate magnetic field of about 100 G produced by a pair of Helmholtz coils in the direction along the horizontal component of Earth's magnetic field was employed during the experiment (Wang et al. 2013).

3. LIFETIME MEASUREMENTS

In the present experiment, the single-step excitation scheme was used. The targeted odd-parity levels of V I were populated from the ground state and some metastable states ranging from 0 to 17,182.073 cm^{-1}. Also, some excited even-parity levels could be reached using the metastable odd levels $3d^3(^4F)4s4p(^3P)$ $z^6G^o_{3/2-13/2}$ ranging from 16,361.489 to 17,136.538 cm^{-1}. Their lifetimes were estimated to range from a fraction of a millisecond to a few seconds using the model described in the next section.

In the measurements, in order to avoid simultaneous excitation of other levels from different metastable states, the exciting wavelength has been carefully chosen from all available excitation pathways. Moreover, the excitation level under study was confirmed by verifying that the observed fluorescence wavelengths were related to this level. The radiation trapping effect, the collisional effect, the flight-out-of-view effect, and the saturation effect which could possibly contribute to the systematic errors of the experimental results have been paid careful attention. The details for checking and eliminating these effects were the same as described in our previous paper (Feng et al. 2011).

To obtain a good signal-to-noise ratio, more than 1000 shots were averaged for each fluorescence decay curve. More than
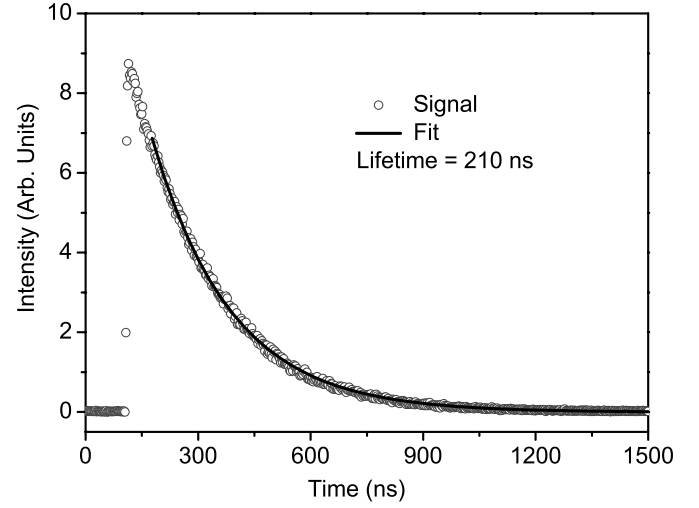
10 curves under different conditions were recorded for each level, and the average value of the lifetimes evaluated from these curves was taken as the final lifetime. The lifetime values shorter than 50 ns were evaluated by fitting the experimental fluorescence decay curve to a convolution of the recorded laser excitation pulse and a pure exponential function. A typical fluorescence decay curve for the 42,245.489 cm^{-1} level with a 12.4(0.9) ns lifetime is shown in Figure 1. For the other longer-lived levels, a least-squares exponential fit procedure was performed to obtain lifetime values. The starting point for the fitting procedure must be chosen carefully to avoid the influence of excitation pulse. A typical fluorescence decay curve for the 31,317.440 cm^{-1} level with a 210(15) ns lifetime obtained by an exponential fit is shown in Figure 2. One can see from Figures 1 and 2 that the fluorescence decay curves were fitted well, and each signal had a good signal-to-noise ratio.

4. HFR+CPOL CALCULATIONS

The Hartree–Fock with relativistic corrections method (HFR) originally developed by Cowan (1981) in which we have included core-polarization (CPOL) effects (see, e.g., Quinet et al. 1999) was used to calculate the lifetimes, the BFs, and the transition probabilities in V I. The intravalence correlation was accounted for by considering the following configurations in the configuration interaction (CI) expansions: $3d^34s^2$ + $3d^34s5s$ + $3d^34s6s$ + $3d^44s$ + $3d^45s$ + $3d^46s$ + $3d^5$ + $3d^44d$ + $3d^45d$ + $3d^46d$ + $3d^34s4d$ + $3d^34s5d$ + $3d^34s6d$ + $3d^34p^2$ + $3d^34d^2$ + $3d^34f^2$ + $3d^34p4f$ + $3d^34s4p^2$ + $3d^24s^24d$ for the even parity and $3d^44p$ + $3d^45p$ + $3d^46p$ + $3d^34s4p$ + $3d^34s5p$ + $3d^34s6p$ + $3d^44f$ + $3d^34s4f$ + $3d^34d4f$ + $3d^24s^24p$ + $3d^24p^3$ for the odd parity. The core-valence correlation was modeled with a polarization potential and a correction to the electric dipole transition operator in which a V IV $3d^2$ ionic core was considered with a dipole polarizability of 2.09 a.u. (Fraga et al. 1976) and a cut-off radius equal to the HFR average radius $\langle r \rangle$ of the $3d$ orbital, i.e., 1.36 a.u.

A 0.8 scaling factor has been applied to the Slater integrals according to a well-established practice in order to consider the effect of far-interacting configurations not explicitly included in the multiconfiguration expansions.

Some radial integrals, considered to be free parameters, were then adjusted with a least-squares optimization program
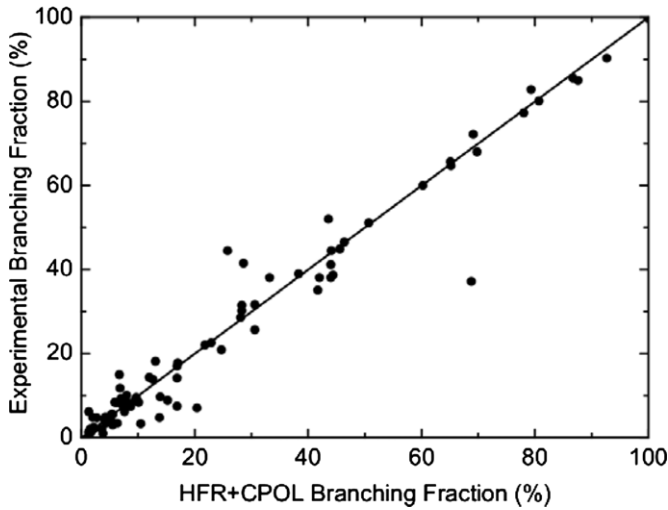
Figure 3. Comparison between the HFR+CPOL branching fractions obtained in this work and those measured by Whaling et al. (1985). The values affected by strong cancellation effects are not plotted (see the text).

Figure 4. Comparison between the corrected log *gf* obtained in this work and the experimental log *gf* determined by Doerr et al. (1985) combining hook and emission measurements. Our values with CF < 0.05 are not plotted (see the text).

minimizing the discrepancies between the calculated Hamiltonian eigenvalues and the experimental energy levels taken from the most recent term analysis of Thorne et al. (2011). More precisely, we followed the fitting procedure described by Thorne et al. (2011) and used their radial parameters as starting values, i.e., the average energies (E_{av}), the direct coulomb interaction integrals within the $3d^N$ (with $N = 3$, 4) cores ($F^2(3d\,3d)$ and $F^4(3d\,3d)$) and the effective interaction parameters (α and β) were fitted as well as the CI Slater integrals between the two odd-parity configurations $3d^44p$ and $3d^34s4p$ ($R^2(3d\,3d, 3d\,4s)$, $R^2(3d\,4p, 4s\,4p)$, and $R^1(3d\,4p, 4p\,4s)$). The average deviations were 130 cm^{-1} for the even parity and 126 cm^{-1} for the odd parity.

Our HFR+CPOL lifetimes are compared with our TR-LIF measurements and previous experimental values in Table 1. Those for which the calculated line strengths of important decay channels (representing more than 10% of the radiative width) are affected by strong cancellation effects, i.e., their cancellation factors (CFs) as defined by Cowan (1981) are less than or equal to 0.05, are marked with an asterisk. Some of the discrepancies between theory and experiment seen in this table can be explained by such a cancellation effect.

In Figure 3, a comparison between the BFs measured by Whaling et al. (1985) and those calculated in this work is shown. The BF values can be affected by strong cancellation effects, i.e., in the formula used for the determination of the theoretical branching fraction, BF$_{ij}$,

$$\mathrm{BF}_{ij} = A_{ij}\tau_i \qquad (1)$$

either the theoretical transition probability, A_{ij}, has a CF less than or equal to 0.05 or the theoretical lifetime is one of those marked with an asterisk in Table 1 or both. These values are not plotted. More precisely, 122 transitions were discarded in this way out of a total of 208. As one can see, except for a few points, a good agreement between both sets is obtained for the strong decay channels (BF > 20%). Indeed strong cancellation effects can still play an indirect role in the few remaining disagreements seen in the figure. For instance, concerning the transition $3d^3(^4F)4s4p$ $z^6D^o_{7/2}$–$3d^4(^5D)4s\,a^6D_{7/2}$, although its CF value is greater than 0.05, it has a HFR+CPOL BF-value equal to 68.8% (CF = 0.07) to be compared to the measurement of Whaling et al. (1985) of
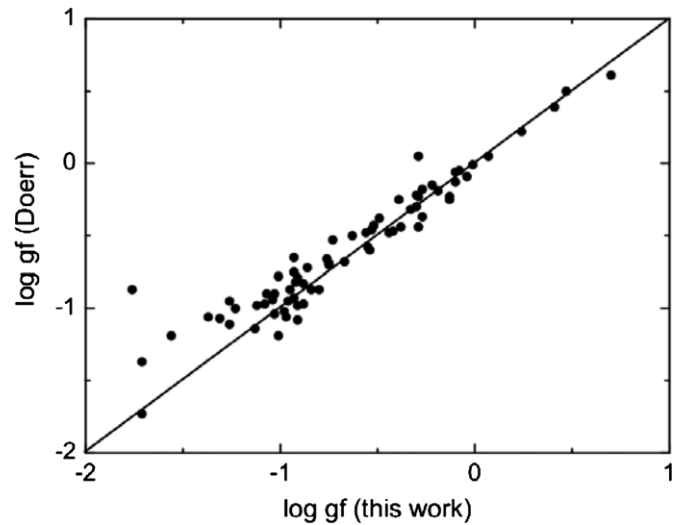
37.2%. This can be explained by the fact that the strongest decay branch from the $3d^3(^4F)4s4p\,z^6D^o_{7/2}$ (that decays to $3d^4(^5D)4s$ $a^6D_{5/2}$), not plotted in the figure, with a measured BF of 41.0% (Whaling et al. 1985) is affected by a very strong cancellation effect (CF = 0.01) giving rise to a weak calculated BF of 6.3% which affects the HFR+CPOL BF-values of all the other decay branches from that level through Equation (1).

In Table 2, the HFR+CPOL weighted transition probabilities (gA), the HFR+CPOL weighted oscillator strengths in the logarithmic scale (log *gf*), and the HFR+CPOL BF are presented for the 784 strongest decay channels (BF ⩾ 1%) of the excited energy levels reported in Table 1. Based on the good agreement between our HFR+CPOL BF values and measurements of Whaling et al. (1985), an improvement on the absolute scale of the radiative rates has been obtained by rescaling our calculated *A* values (and consequently our calculated *f* values). The corrected *A* values have been extracted by combining the available experimental lifetimes (given just below the corresponding upper level of the transition) with the HFR+CPOL BF values using Equation (1). These corrected transition probabilities and oscillator strengths are given in the seventh and eighth columns of the table. In the last column, the CF is also reported. A CF value less than 0.05 indicates that the transition probability is affected by a strong cancellation effect and therefore should be taken with care.

The accuracy of our semi-empirical *f* values can be further assessed by comparing with those determined by Doerr et al. (1985) combining hook and emission measurements. In Figure 4, we plot the log *gf* of Doerr et al. with respect to our corrected values discarding the 9 transitions (out of 81) for which the CF values are less than 0.05. A good agreement is found with an average difference between these two sets of 0.07 dex (the standard deviation being 0.16 dex). The remaining strong disagreement seen for the transition $3d^3(^4P)4s4p(^3P)$ $w^4D^o_{7/2}$–$3d^4(^5D)4s\,a^6D_{7/2}$ (−0.87 in Doerr et al. compared to −1.76 in this work) is probably due to cancellation effects. Indeed, the CF value of 0.06 is close to threshold (0.05) and our HFR+CPOL lifetime of the upper level of that transition used to calculate the BF value is affected by strong cancellation effects (see Table 1).

Table 1
Comparison between Theoretical and Experimental Lifetimes of V I Energy Levels

Level[a]				$\lambda_{Exc.}$	$\lambda_{Obs.}$	Lifetime (ns)		
Configuration	Term	J	E (cm^{-1})	(nm)	(nm)	This Expt.	Prev. Expt.	HFR
$3d^3(^4F)4s4p(^3P)$	z^6D^o	1/2	18085.952				390(40)[b]	361*
		3/2	18126.250				395(40)[b]	389*
		5/2	18198.091				395(40)[b]	442*
		7/2	18302.280				385(40)[b]	542
		9/2	18438.044				370(40)[b]	492*
$3d^3(^4F)4s4p(^3P)$	z^4D^o	1/2	20606.467				86(3)[b]	87.9*
		3/2	20687.769				83(3)[b]	89.5*
		5/2	20828.481				89(3)[b]	91.6*
		7/2	21032.503				92.5(3)[b]	93.8*
$3d^3(^4F)4s4p(^3P)$	z^4G^o	5/2	21841.421				183(3)[b]	239*
		7/2	21963.437				179(3)[b] 12.4(1.9)[c]	234*
		9/2	22121.079				174(3)[b]	227*
		11/2	22313.832				168(3)[b] 12.0(1.8)[c]	220*
$3d^3(^4F)4s4p(^3P)$	z^4F^o	3/2	23088.074				145(3)[b]	187*
		5/2	23210.560				132(3)[b]	175*
		7/2	23353.135				128(4)[b]	173*
		9/2	23519.872				133(4)[b] 7.0(1.4)[c]	174*
$3d^4(^5D)4p$	z^4P^o	1/2	24770.673				24(1)[b]	23.1
		3/2	24915.151				24(1)[b] 9.5(2.0)[d]	23.1
		5/2	25131.002				25(1)[b]	23.0
$3d^4(^5D)4p$	y^4F^o	3/2	25930.544				14.3(0.5)[b] 14.3(1.0)[e]	13.3
		5/2	26004.234				14.4(0.5)[b] 15.0(1.1)[e]	13.3
		7/2	26122.094				17.6(0.5)[b] 18.2(1.3)[e]	22.4
		9/2	26171.918				19.2(0.5)[b] 21.0(1.5)[e]	14.6
$3d^3(^4F)4s4p(^3P)$	z^2G^o	7/2	26021.907				67(3)[b] 71(5)[e]	26.1
		9/2	26344.902				49(3)[b]	96.8
$3d^4(^5D)4p$	y^4D^o	1/2	26182.637				12.3(0.5)[b] 12.7(0.9)[e] 12.3(0.7)[f]	11.9
		3/2	26249.476				12.3(0.5)[b] 12.9(0.9)[e] 11.9(0.7)[f]	11.9
		5/2	26352.634				12.4(0.5)[b] 13.3(0.9)[e] 12.4(0.7)[f]	12.1
		7/2	26480.286				12.5(0.5)[b] 13.8(1.0)[e] 12.2(0.7)[f]	13.2
$3d^4(^5D)4p$	y^6D^o	1/2	26397.633				7.7(0.5)[b] 8.0(0.4)[f]	7.06
		3/2	26437.754				7.8(0.5)[b] 8.1(0.4)[f]	7.05
		5/2	26505.953				7.9(0.5)[b] 7.9(0.4)[f]	7.04
		7/2	26604.807	377.823	410	7.8(0.5)	7.8(0.5)[b] 8.0(0.4)[f]	7.05
		9/2	26738.323				7.9(0.5)[b] 7.8(0.4)[f] 9.3(1.4)[c]	7.16
$3d^3(^4F)4s4p(^3P)$	z^2F^o	5/2	27187.747	367.813	368	494(46)		617
$3d^3(^4P)4s4p(^3P)$	x^6D^o	1/2	28313.626	353.187	382	36.4(2.5)		26.5
		3/2	28368.753	354.216	381	36.5(2.6)		26.5
		5/2	28462.177	355.382	380	37.7(2.6)		26.6
		7/2	28595.637	356.600	379	38.7(2.7)		26.7
		9/2	28768.142	377.976	379	39.7(2.8)		27.0
$3d^3(^4P)4s4p(^3P)$	y^6P^o	3/2	29202.790	369.133	371	6.4(0.4)		6.05
		5/2	29296.430	368.417	371	6.9(0.5)		6.06
		7/2	29418.119	367.675	371	7.0(0.5)		6.06

Table 1
(Continued)

Level[a]				$\lambda_{\text{Exc.}}$	$\lambda_{\text{Obs.}}$	Lifetime (ns)		
Configuration	Term	J	E (cm^{-1})	(nm)	(nm)	This Expt.	Prev. Expt.	HFR
$3d^3(^4P)4s4p(^3P)$	y^4P^{o}	1/2	30021.627	358.830	462	49.3(3.5)		51.1*
		3/2	30094.585	357.892	468	51.2(3.6)		52.9*
		5/2	30120.823	359.590	464	55.8(3.9)		59.9*
$3d^3(^2G)4s4p(^3P)$	y^4G^{o}	5/2	30635.580	326.418	329	76.4(4.2)	74.0(5)[g]	8.69
		7/2	30694.344	327.257	327		87(6)[g]	10.6
		9/2	30771.732	328.425	328		105(10)[g]	13.8
		11/2	30864.279	351.624	329	142(10)		19.0
$3d^3(^2G)4s4p(^3P)$	x^4F^{o}	3/2	31200.152	321.929	442	232(16)		185*
		5/2	31229.014	323.566	444	208(15)		158*
		7/2	31268.091	323.158	443	207(15)		166*
		9/2	31317.440	325.050	442	210(15)		177
$3d^3(^4F)4s4p(^1P)$	x^4G^{o}	5/2	31397.822				3.6(5)[b]	4.23
		7/2	31541.167				3.6(5)[b]	3.89
		9/2	31721.780				3.6(5)[b]	3.59
		11/2	31937.131				3.6(5)[b]	3.37
$3d^3(^2P)4s4p(^3P)$	x^4D^{o}	3/2	32456.581	309.414	417	90.6(6.3)		59.3*
$3d^3(^2G)4s4p(^3P)$	y^2G^{o}	9/2	33306.943	323.812	446	40.1(3.3)		117*
		7/2	33360.280	323.253	445	59.4(4.2)		103*
$3d^3(^4P)4s4p(^3P)$	w^4D^{o}	7/2	34127.921	315.426	393	16.7(1.2)		14.0*
$3d^3(^4F)4s4p(^1P)$	v^4D^{o}	3/2	34537.299	309.433	383	18.6(1.3)		15.3
		5/2	34619.598	309.519	386	11.5(0.8)		11.5
$3d^3(^2D)4s4p(^3P)$	u^4D^{o}	1/2	35013.259	376.832	285	17.4(1.2)		12.9
		3/2	35092.518	374.819	572	18.7(1.3)		12.8
		5/2	35224.990	377.227	283	21.4(1.5)		13.0
$3d^3(^4P)4s4p(^3P)$	y^4S^{o}	3/2	36408.402	357.202	376	10.2(0.7)		22.9*
$3d^4(a^3F)4p$	$^2G^{\text{o}}$	7/2	36461.282	360.418	394	17.8(1.2)		16.3
		9/2	36538.569	359.417	389	17.1(1.2)		17.0
$3d^4(a^3P)4p$	$^2P^{\text{o}}$	1/2	36477.728	356.319	556	6.6(0.5)		26.9
		3/2	36580.427	355.020	291	5.5(0.4)		36.7*
$3d^3(^2D)4s4p(^3P)$	x^4P^{o}	1/2	36695.612	368.310	463	38.7(2.7)		25.9
		3/2	36814.827	366.701	464	33.0(2.3)		22.4*
		5/2	36611.845	370.717	355	43.8(3.1)		30.6*
$3d^3(^4P)4s4p(^3P)$	x^2D^{o}	5/2	36700.768	369.498	388	43.7(3.1)		42.9*
$3d^3(^2H)4s4p(^3P)$	w^4G^{o}	7/2	36822.878	354.054	385	37.5(3.0)		147
$3d^4(a^3F)4p$	x^2F^{o}	5/2	36766.041	353.484	271	5.7(0.4)		18.3
		7/2	36925.893	352.767	369	9.5(0.7)		13.0
$3d^4(^3H)4p$	v^2G^{o}	7/2	37174.691	365.630	381	19.5(1.4)		16.8
		9/2	37361.951	377.794	446	13.9(1.0)		11.6
$3d^4(^3H)4p$	z^2I^{o}	11/2	37530.314	378.362	444	20.2(1.4)		14.4
$3d^4(a^3P)4p$	t^4D^{o}	1/2	37757.309	264.849	354		5.3(0.4)[g]	5.23
		5/2	37959.695	369.451	370	5.6(0.4)		7.21
		7/2	38115.684	264.604	353		5.6(0.4)[g]	5.19
$3d^4(^3H)4p$	x^2H^{o}	9/2	38123.795	367.225	313	3.3(0.2)		14.2
		11/2	38220.663	368.731	430	14.3(1.0)		13.9
$3d^4(^3H)4p$	x^4H^{o}	7/2	38245.829	365.586	422	8.3(0.6)		7.46
		11/2	38405.067	366.240	426	8.1(0.6)		7.32
$3d^3(^2H)4s4p(^3P)$	u^2G^{o}	9/2	38529.830	364.575	423	8.5(0.6)		48.0*
$3d^4(a^3P)4p$	w^4P^{o}	3/2	39248.928	324.297	417	7.3(0.5)		6.13
		5/2	39422.745	325.659	350	7.0(0.4)		5.79
$3d^4(a^3F)4p$	u^4F^{o}	3/2	39266.680	324.776	424	9.2(0.6)	8.7(0.6)[g]	6.72
		5/2	39300.537	255.341	424		9.4(0.7)[g]	6.68
		7/2	39341.784	256.289	423		9.5(0.7)[g]	6.76
		9/2	39391.079	353.476	271	5.7(0.4)	9.6(0.7)[g]	6.89
$3d^4(a^3F)4p$	s^4D^{o}	3/2	39935.176	318.912	412	6.4(0.4)		5.25
$3d^4(^3H)4p$	u^4G^{o}	5/2	39962.150	320.037	344	27.6(1.1)		5.76
$3d^4(a^3P)4p$	v^2D^{o}	5/2	40119.218	317.051	396	14.0(0.5)		10.8
$3d^4(^3G)4p$	$^2F^{\text{o}}$	5/2	40325.790	313.977	405	9.7(0.4)		10.3
$3d^4(^3G)4p$	t^4F^{o}	3/2	41389.644	314.934	412	8.0(0.6)		8.09
		5/2	41429.042	377.088	470	24.9(1.7)		7.88
		9/2	41599.436	377.420	488	10.8(0.7)		7.21
$3d^4(^3G)4p$	t^2G^{o}	7/2	41436.610	377.540	300	130(13)		8.34
		9/2	41539.185	376.815	326	10.1(0.7)		7.94
$3d^4(^3G)4p$	t^4G^{o}	5/2	41654.726	325.073	407	7.9(0.6)		6.79
				368.920	369	7.3(0.5)		

Table 1
(Continued)

Configuration	Term	J	E (cm^{-1})	$\lambda_{Exc.}$ (nm)	$\lambda_{Obs.}$ (nm)	This Expt.	Prev. Expt.	HFR
$3d^3(^4P)4s4p(^1P)$	v^4P^o	1/2	41751.931	310.489	377	7.4(0.5)		7.41*
		5/2	42009.912	378.245	407	7.9(0.6)		7.76
$3d^4(^3D)4p$	u^2F^o	5/2	41950.393	364.489	322	12.0(1.2)		11.4
		7/2	42020.903	371.511	399	7.5(0.5)		10.9
$3d^3(^4P)4s4p(^1P)$	r^4D^o	1/2	41928.473	238.501	309		7.3(0.5)^g	8.10
		3/2	41999.261	310.804	378	7.7(0.5)		8.08*
				378.398	308	7.7(0.5)		
		7/2	42245.489	308.404	376	12.4(0.9)		9.08
$3d^4(^5D)5p$	$^6F^o$	5/2	42172.123	378.102	371	42.8(3.0)		49.1*
		7/2	42236.621	377.846	298	16.5(1.2)		84.8
$3d^3(^4F)4s5p$	$^6D^o$	7/2	44026.568	370.761	339	10.8(1.0)		53.9*
$3d^34s(^5F)4d$	f^6P	7/2	44083.247	363.496	364	6.8(0.5)		7.25
$3d^34s(^5F)4d$	^6F	9/2	44205.606	361.887	362	6.4(0.5)		6.57
$3d^3(^2F)4s4p(^3P)$	p^4F^o	5/2	45688.309	313.610	406	9.8(0.4)		10.4
$3d^3(^4F)4s5p$	o^4D^o	3/2	45762.309	312.884	403	10.8(0.8)		6.98
				312.975	401	10.9(0.8)		
		5/2	45838.082	319.251	401	9.0(0.4)		6.86*
$3d^3(^2F)4s4p(^3P)$	r^4G^o	5/2	46052.702	217.142	317	9.5(0.7)		8.27
$3d^4(^3D)4p$	t^4P^o	3/2	46862.786	214.016	377	4.7(0.3)		3.89

Notes. The excitation wavelength $\lambda_{Exc.}$ is in vacuum.
[a] Thorne et al. (2011).
[b] Whaling et al. (1985).
[c] Roberts et al. (1973).
[d] Childs et al. (1979)
[e] Rudolph & Helbig (1982).
[f] Doerr et al. (1985).
[g] Xu et al. (2006).
* Strong cancellation effects on lifetime (see the text).

Table 2
Transition Probabilities (gA), Oscillator Strengths (log gf) and Branching Fractions (BF) for the Strongest Decay
Channels Depopulating the Levels for which the Lifetime has been Measured in V I

Upper Level[a]	Lower Level[a]	λ[a] (nm)	gA (s^{-1})	log gf	BF (%)	gA_{cor}[b] (s^{-1})	log gf_{cor}[b]	CF[c]
18085.952 (o) 1/2	2112.282 (e) 1/2	625.8571	9.00E+05	−2.28	16.2	8.33E+05	−2.31	0.04
$\tau = 390(40)^d$ ns	2153.221 (e) 3/2	627.4652	4.63E+06	−1.56	83.6	4.29E+06	−1.60	0.08
18126.250 (o) 3/2	2112.282 (e) 1/2	624.2822	2.89E+06	−1.77	28.1	2.85E+06	−1.78	0.04
$\tau = 395(40)^d$ ns	2153.221 (e) 3/2	625.8822	5.02E+05	−2.53	4.9	4.95E+05	−2.54	0.05
	2220.156 (e) 5/2	628.5160	6.88E+06	−1.39	66.9	6.78E+06	−1.40	0.08
18198.091 (o) 5/2	2153.221 (e) 3/2	623.0798	2.71E+06	−1.80	20.0	3.03E+06	−1.75	0.02
$\tau = 395(40)^d$ ns	2220.156 (e) 5/2	625.6900	4.35E+06	−1.59	32.1	4.87E+06	−1.54	0.07
	2311.369 (e) 7/2	629.2824	6.50E+06	−1.41	47.9	7.27E+06	−1.36	0.08
18302.280 (o) 7/2	2220.156 (e) 5/2	621.6364	9.34E+05	−2.27	6.3	1.31E+06	−2.12	0.01
$\tau = 385(40)^d$ ns	2311.369 (e) 7/2	625.1823	1.02E+07	−1.23	68.8	1.43E+07	−1.08	0.07

Notes. The energy levels are labeled by their values, parities ("e" for even and "o" for odd), and total quantum number J. The wavelengths
are determined from the energy levels of this reference by the Ritz formula and are given in air above 200 nm.
[a] Thorne et al. (2011).
[b] Determined by a combination of the experimental lifetime (reported below the upper level) and the HFR+CPOL BF.
[c] Cancellation factor (CF) as defined in Cowan (1981). The transition probability for which the CF is less than 0.05 is affected by a
strong cancellation effect and should be taken with caution.
[d] Whaling et al. (1985).
[e] This work.
[f] Xu et al. (2006).

(This table is available in its entirety in a machine-readable form in the online journal. A portion is shown here for guidance regarding
its form and content.)

5. RESULTS AND DISCUSSION

In this paper, radiative lifetimes for 79 V I levels from
26,604.807 to 46,862.786 cm^{-1} belonging to the configurations
$3d^34s4p$, $3d^44p$, $3d^34s5p$, $3d^45p$, and $3d^34s4d$ have been mea-
sured and presented in Table 1. The quoted error bars consist of
both the statistical uncertainties from different recordings and
the systematic errors from the fitting processes. The lifetime

values fall in the range from 3.3 to 494 ns with the uncertainties no more than $\pm 10\%$. To the best of our knowledge, 75 lifetimes of V I levels were measured for the first time.

Our new measurements for the levels $y^6D^o_{7/2}$, $y^4G^o_{5/2}$, and $u^4F^o_{3/2}$ are supported by previous TR-LIF values (Whaling et al. 1985; Doerr et al. 1985; Xu et al. 2006). An exception is the case of the level $u^4F^o_{9/2}$ for which our experimental value is slightly closer to our HFR+CPOL calculation than the measurement of Xu et al. (2006).

Although our HFR+CPOL calculation supports our measurements and previous experimental lifetimes in several instances, important disagreements still remain that cannot be explained by cancellation effects. A noticeable example is given by the y^4G^o multiplet for which the experimental lifetimes range from 74.0(5.0) ns to 142(10) ns and the HFR+CPOL values are an order of magnitude shorter, ranging from 8.69 ns to 19.0 ns. In that case, line blends seem unlikely to be the cause of the observed differences because the experimental lifetimes of all the levels of this multiplet are of the same order of magnitude. Actually, a strong intermediate coupling mixing occurs for this term between the basis vectors $3d(^2G)4s4p\ ^4G^o$ (with contributions ranging from 57% for $J = 5/2$ to 73% for $J = 11/2$) and $3d(^4F)4s4p\ ^4G^o$ (with contributions ranging from 20% for $J = 11/2$ to 31% for $J = 5/2$). A sensitivity test of the calculated lifetimes to the eigenvector LS compositions shows that a decrease of a factor of about two of the $3d(^4F)4s4p\ ^4G^o$ basis vector contributions (i.e., the contributions now ranging from 10% for $J = 11/2$ to 13% for $J = 5/2$) to the y^4G^o term increases all the calculated lifetimes by a factor of about four. Although this change is in the right direction, it is still not enough to reach a good theory–experiment agreement but itdoes show the rather high sensitivity of the computed radiative lifetimes to the change in eigenvector compositions.

In conclusion, given the good agreement between the experimental (Whaling et al. 1985) and our calculated BF values (see Figure 3) and the general consistencies shown in Table 1 among

the available laser measurements (this work and Whaling et al. 1985; Rudolph & Helbig 1982; Doerr et al. 1985; Xu et al. 2006), the corrected transition probabilities given in Table 2 are the ones that are recommended to the users. Moreover, this is further supported by the good agreement found between our recommended oscillator strengths and the f values determined by Doerr et al. (1985; see Figure 4).

REFERENCES

Asplund, M., Grevesse, N., Sauval, J. A., & Scott, P. 2009, ARA&A, 47, 481
Childs, W. J., Poulsen, O., Goodman, L. S., & Crosswhite, H. 1979, PhRvA, 19, 168
Cowan, R. D. 1981, The Theory of Atomic Structure and Spectra (Berkeley, CA: Univ. California Press)
Den Hartog, E. A., Bilty, K. A., & Lawler, J. E. 2011, JPhB, 44, 055001
Doerr, A., Kock, M., Kwiatkowski, M., Werner, K., & Zimmermann, P. 1985, JQSRT, 33, 55
Feng, Y. Y., Jiang, L. Y., Wang, Q., et al. 2011, MNRAS, 418, 998
Feng, Y. Y., Zhang, W., Ning, L., et al. 2010, JPhB, 43, 225001
Fraga, S., Karwowski, J., & Saxena, K. M. S. 1976, Handbook of Atomic Data (Amsterdam: Elsevier)
Larsson, J. 1994, PhysS, 49, 173
Meléndez, J., Asplund, M., Gustafsson, B., & Yong, D. 2009, ApJL, 704, L66
Quinet, P., Palmeri, P., Biémont, E., et al. 1999, MNRAS, 307, 934
Ramírez, I., Meléndez, J., & Asplund, M. 2014, A&A, 561, A7
Roberts, J. R., Andersen, T., & Sørensen, G. 1973, ApJ, 181, 587
Rudolph, J., & Helbig, V. 1982, JPhB, 15, L599
Thorne, A. P., Pickering, J. C., & Semeniuk, J. 2011, ApJS, 192, 11
Wang, Q., Jiang, L. Y., Jiang, H. M., et al. 2013, JPhB, 46, 045003
Whaling, W., Hannaford, P., Lowe, R. M., Biémont, E., & Grevesse, N. 1985, A&A, 153, 109
Xu, H. L., Jiang, Z. K., & Lundberg, H. 2006, JOSAB, 23, 2597
Zhang, W., Feng, Y. Y., Xu, J., et al. 2010, JPhB, 43, 205005